

Mössbauer and magnetic studies of Ti^{4+} -substituted Ni-Zn ferrites

R. C. Srivastava, D. C. Khan, and A. R. Das*

Department of Physics, Indian Institute of Technology, Kanpur 208 016, Uttar Pradesh, India.

(Received 8 December 1989; revised manuscript received 12 March 1990)

In the present work we make Mössbauer and magnetization studies of the Ti^{4+} -substitution effect in the $\text{Ni}_{1-y}\text{Zn}_y\text{Fe}_2\text{O}_4$ ferrite ($y=0.3$ and 0.4). In this range the Mössbauer spectra are not relaxed and may be used to get an insight into the Ti^{4+} distribution process as well as the microscopic mechanism of anomalous magnetization. It is observed that $H_{\text{eff}}(B)$ remains almost constant and $H_{\text{eff}}(A)$ decreases as the concentration of Ti^{4+} ions increases in the lattice. Evidently, Ti^{4+} ions occupy only the octahedral B site. The nonlinear behavior of magnetization with the increase of Ti^{4+} ions is explained by the presence of canted spin structure. It is found that the change of the canting angle is basically due to the change in the exchange constant $J_{\text{Ni}^{2+}(B)\text{-Ni}^{2+}(B)}$. This is a consequence of the positional readjustment of various cations after the entry of Ti^{4+} ions into the lattice.

I. INTRODUCTION

Ti^{4+} -substituted Ni-Zn ferrite systems have recently been the focus of attention of a number of workers.¹⁻⁶ Khan and co-workers^{1,2} found a very interesting behavior of saturation magnetization in Ti^{4+} -substituted $\text{Ni}_{0.3}\text{Zn}_{0.7}\text{Fe}_2\text{O}_4$ ferrite. They observed that there is an unexpected dip in the saturation magnetization curve at Ti^{4+} concentration of 0.03 per formula unit. They interpreted this as an effect of the distribution of the Ti^{4+} ions between A and B sites. Ti^{4+} ions enter at A site up to a Ti^{4+} concentration of 0.03 per formula unit and afterwards to the B site also. Khan's assertion on this type of anomalous behavior of magnetization as a function of Ti^{4+} concentration in Ni-Zn ferrite systems was corroborated by the experiments of Das, Ananthan, and Khan³ for a wide range of substituted Ni-Zn ferrites (substituents: Ti^{4+} , Zr^{4+} , Nb^{5+} , and Sn^{4+} ; and Zn concentrations: 0.3, 0.5, and 0.7 per formula unit).

The efforts of Khan and Misra² to use Mössbauer results for the interpretation of the anomaly were not fruitful since the spectra were relaxed. In the present work we studied the effect of Ti^{4+} substitution in $\text{Ni}_{1-y}\text{Zn}_y\text{Fe}_2\text{O}_4$ ferrite ($y=0.3$ and 0.4), where the Mössbauer spectra are not relaxed, with a view to use Mössbauer information for getting insight into the Ti^{4+} distribution process as well as the microscopic magnetization mechanism. The Ti^{4+} concentration range was chosen to keep the system in the anomalous dip zone of the experiments of Khan and co-workers.^{1,2} Baijal and co-workers^{4,5} studied $\text{Zn}_{0.25}\text{Ni}_{0.75+x}\text{Ti}_x\text{Fe}_{2-2x}\text{O}_4$ ($x=0.0$ to 0.5 in steps of 0.1) ferrite and Puri, Atmaram, and Rao⁶ studied $\text{Zn}_y\text{Ni}_{1+x-y}\text{Ti}_x\text{Fe}_{2-2x}\text{O}_4$ ($y=0.1$ and 0.5 ; $x=0.1-0.9$ in steps of 0.2) ferrite. Their work did not yield any anomalous dip in the saturation magnetization curve as observed by Khan and co-workers.^{1,2} Contrary to the results of Khan and co-workers^{1,2} and Das, Ananthan, and Khan,³ the results of Baijal and co-workers^{4,5} show that Ti^{4+} ions occupy the B site first up to the Ti^{4+} concentration of 0.3 and beyond this concen-

tration it occupies both A and B sites. Thus the occupation of tetravalent nonmagnetic cations, particularly at low concentrations, and their effects on microscopic magnetic processes, such as exchange, remains an open question.

II. EXPERIMENT

For the present study the ferrite samples were prepared in the oxidizing atmosphere by the solution route technique. X-ray diffraction of the samples was done on a Siefert x-ray diffractometer using Cu as target. The x-ray diffraction pattern of the samples confirmed the presence of single spinel phase. The magnetization measurements were made on a 150A vibrating sample magnetometer supplied by Princeton Applied Research Corporation, U.S.A. The Mössbauer spectra of the samples were recorded by using an ND-62 multichannel analyzer. A 25-mCi ^{57}Co -in-Rh source obtained from E. I. du Pont, U.S.A. was used.

III. STUDY OF MÖSSBAUER HYPERFINE PARAMETERS

Mössbauer spectra of samples were recorded at room temperature and at liquid-nitrogen temperature. They show a well-defined Zeeman pattern consisting of two separate sextets, due to Fe^{3+} ions at A and B sites. Mössbauer spectra of Ti^{4+} -substituted $\text{Ni}_{0.7}\text{Zn}_{0.3}\text{Fe}_2\text{O}_4$ at 295 and 77 K are shown in Figs. 1 and 2, respectively. The corresponding spectra for Ti^{4+} -substituted $\text{Ni}_{0.6}\text{Zn}_{0.4}\text{Fe}_2\text{O}_4$ have qualitatively similar features.

The isomer shift of Fe^{3+} ions (with respect to sodium nitroprusside) at the tetrahedral site $\Delta_{\text{IS}}(A)$ and at the octahedral site $\Delta_{\text{IS}}(B)$ shows no significant change with Ti^{4+} concentration. The values of isomer shift in Ti^{4+} -substituted $\text{Ni}_{0.7}\text{Zn}_{0.3}\text{Fe}_2\text{O}_4$ ferrite at 295 and 77 K with different concentration of Ti^{4+} ions are shown in Fig. 3. The weighted average values of isomer shift at A and B sites at 295 K are 0.533 ± 0.002 and 0.615 ± 0.002 mm/sec,

respectively. At 77 K, the weighted average values of isomer shift at *A* and *B* sites are 0.719 ± 0.002 and 0.840 ± 0.002 mm/sec, respectively.

In the Ti^{4+} -substituted $Ni_{0.6}Zn_{0.4}Fe_2O_4$ ferrite system, too, the isomer shift of Fe^{3+} ions at *A* and *B* sites does not show any significant change with Ti^{4+} concentration. The weighted average values of $\Delta_{IS}(A)$ and $\Delta_{IS}(B)$ at 295 K are 0.542 ± 0.003 and 0.642 ± 0.003 mm/sec, respectively, whereas the respective values at 77 K are 0.734 ± 0.003 and 0.872 ± 0.003 mm/sec.

Our results indicate that the *s*-electron density at the Fe^{3+} nucleus is not affected by Ti^{4+} substitution, since the isomer shift, for a particular nuclear transition of the Mössbauer source, is dependent only on the *s*-electron charge density of the absorber. The values of the isomer shift at *A* and *B* sites show that iron is in the Fe^{3+} state.⁷ The result $\Delta_{IS}(A) < \Delta_{IS}(B)$ is in agreement with the results of other workers.^{8,9} This is interpreted as being due to the large bond separation $Fe^{3+}-O^{2-}$ for the octahedral ions as compared to that of the tetrahedral ions. Due to smaller overlapping of orbitals of Fe^{3+} and O^{2-} ions, the covalency effect is small, and hence the isomer shift is large at the octahedral sites. It is also found that the isomer shift at 77 K is larger than its value at 295 K. This increased value of isomer shift at 77 K is due to the thermal red shift between the source at 295 K and the ab-

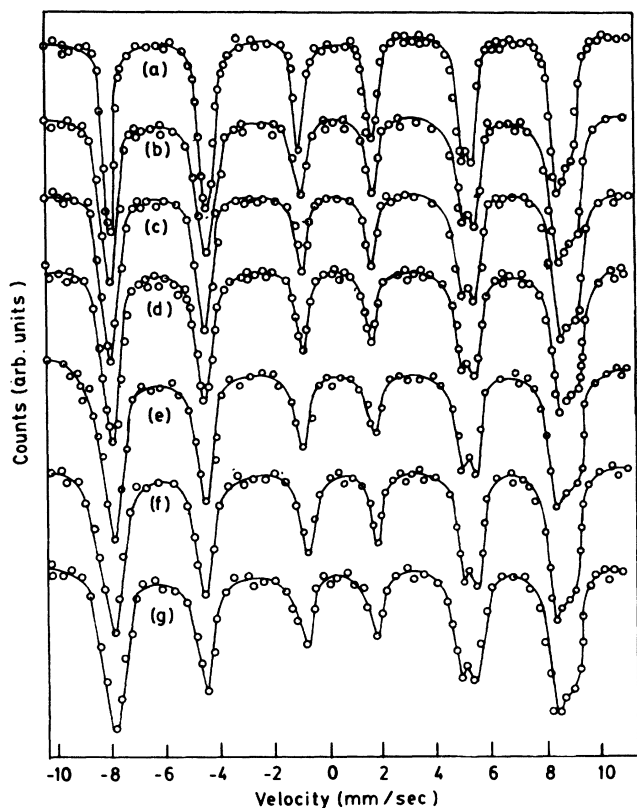


FIG. 1. Mössbauer spectra of $Ni_{0.7+x}Zn_{0.3}Ti_xFe_{2-2x}O_4$ at room temperature. Curve (a), $x=0.000$; curve (b), $x=0.002$; curve (c), $x=0.01$; curve (d), $x=0.016$; curve (e), $x=0.032$; curve (f), $x=0.05$; curve (g), $x=0.08$.

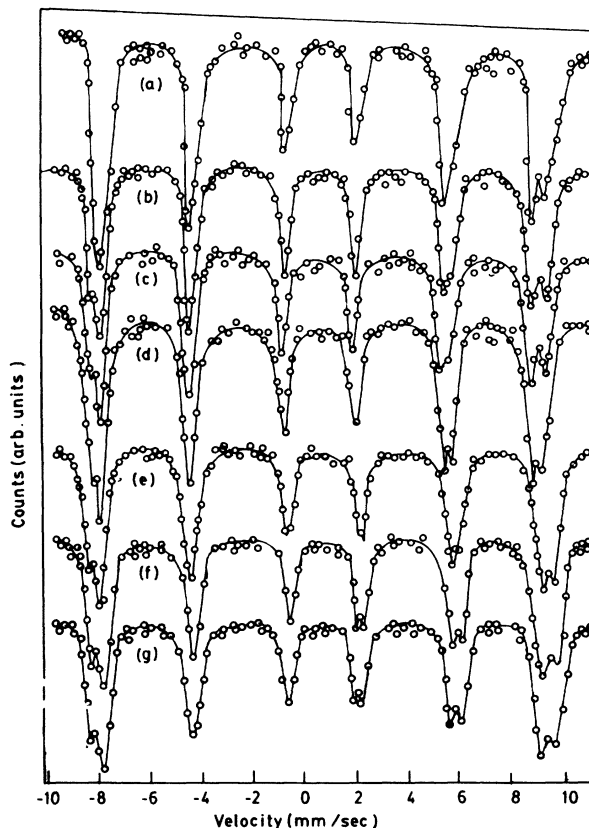


FIG. 2. Mössbauer spectra of $Ni_{0.7+x}Zn_{0.3}Ti_xFe_{2-2x}O_4$ at 77 K. Curve (a), $x=0.000$; curve (b), $x=0.002$; curve (c), $x=0.01$; curve (d), $x=0.016$; curve (e), $x=0.032$; curve (f), $x=0.05$; curve (g), $x=0.08$.

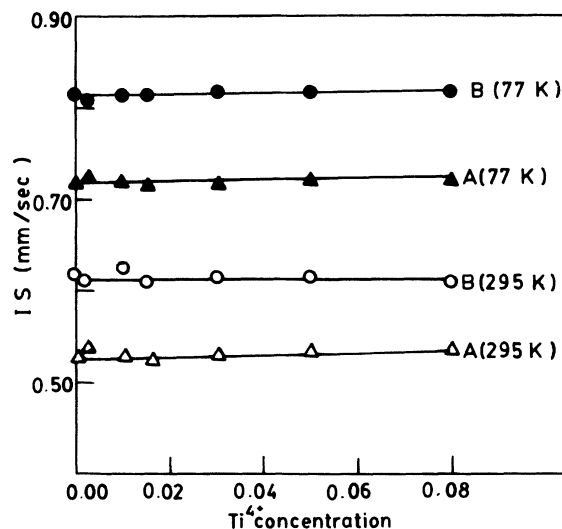


FIG. 3. Variation of isomer shift with Ti^{4+} concentration in $Ni_{0.7+x}Zn_{0.3}Ti_xFe_{2-2x}O_4$ ferrite.

sorber at 77 K.^{10,11}

In all the samples exhibiting a Zeeman hyperfine pattern, no quadrupole splitting was observed within the experimental error for both *A* and *B* sites. This lack of an observable quadrupole splitting in ferrites has been mistakenly interpreted as signifying the absence of an electric field gradient (EFG). That such is not the case is clearly shown by the spectra which no longer display a Zeeman pattern (Mössbauer spectra of $\text{Ni}_{1-y}\text{Zn}_y\text{Fe}_2\text{O}_4$, $0.7 \leq y \leq 1.0$ by Daniels and Rosencwaig¹²). The zero quadrupole splitting in such ferrites may be explained as being due to the presence of chemical disorder. The chemical disorder will produce a distribution of electric field gradient of varying magnitude, direction, sign, and symmetry. The resulting distribution of the quadrupole shift, given by Matthias, Schneider, and Steffen,¹³ is

$$|\Delta E_Q| = \frac{1}{2} |\Delta E_{Q0}| (3 \cos^2 \theta - 1), \quad (1)$$

where $|\Delta E_{Q0}|$ is the magnitude of the shift when the magnetic interaction tends to zero and θ is the angle between the axially symmetric EFG and the magnetic field direction. This distribution will produce a noticeable broadening of the individual lines of Zeeman pattern. Because of the overall cubic symmetry of the spinel ferrite and the randomness of chemical disorder, the above equation will give rise to approximately equal probability for small quadrupole splitting of opposite sign. Hence the centers of the Zeeman lines will not change. This will then result in no net observable quadrupole splitting.

In Ti^{4+} -substituted $\text{Ni}_{0.7}\text{Zn}_{0.3}\text{Fe}_2\text{O}_4$ ferrite, at 295 K, the variation of H_{eff} at *A* and *B* sites with Ti^{4+} concentration is shown in Fig. 4. From the graph it is observed that there is no significant change in $H_{\text{eff}}(B)$ and it remains almost constant at a value of 495 ± 1 kOe. $H_{\text{eff}}(A)$, on the other hand, decreases from 487 ± 1 to 483 ± 1 kOe as the concentration of Ti^{4+} increases from $x=0.00$ to 0.08. A similar behavior of $H_{\text{eff}}(A)$ and $H_{\text{eff}}(B)$ with Ti^{4+} concentration is observed at 77 K also

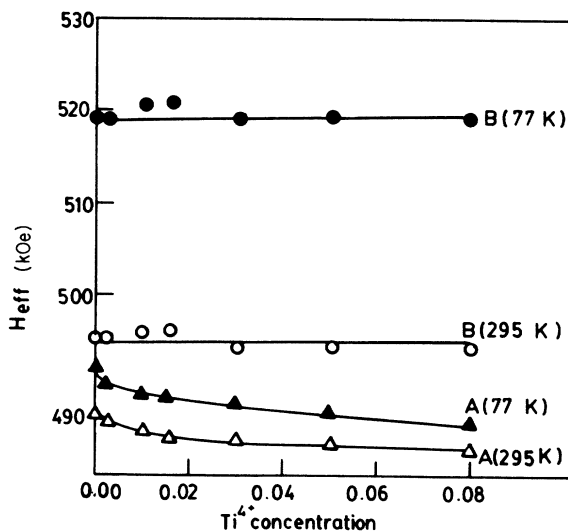


FIG. 4. Variation of hyperfine magnetic field with Ti^{4+} concentration in $\text{Ni}_{0.7+x}\text{Zn}_{0.3}\text{Ti}_x\text{Fe}_{2-2x}\text{O}_4$ ferrite.

(Fig. 4). Here $H_{\text{eff}}(B)$ remains almost constant at 519 ± 1 kOe, whereas $H_{\text{eff}}(A)$ decreases from 492 ± 1 to 486 ± 1 kOe as the concentration of Ti^{4+} ions increases from $x=0.00$ to 0.08. For the zero concentration of Ti^{4+} the values of H_{eff} at the two sublattices at 295 and 77 K are in excellent agreement with the values reported in the literature.¹²

In Ti^{4+} -substituted $\text{Ni}_{0.6}\text{Zn}_{0.4}\text{Fe}_2\text{O}_4$ ferrite also there is no significant change in $H_{\text{eff}}(B)$ with Ti^{4+} concentration and it remains almost constant at a value of 446 ± 1 kOe. $H_{\text{eff}}(A)$, on the other hand, decreases from 480 ± 1 to 474 ± 1 kOe as the concentration of Ti^{4+} ions increases from $x=0.00$ to 0.08. A similar behavior of $H_{\text{eff}}(A)$ and $H_{\text{eff}}(B)$ with Ti^{4+} concentration is observed at 77 K also. At 77 K, $H_{\text{eff}}(B)$ remains constant at a value of 518 ± 1 kOe, whereas $H_{\text{eff}}(A)$ decreases from 506 ± 1 to 497 ± 1 kOe.

The variation of effective magnetic field at the two sublattices could be understood on the basis of Néel's molecular-field theory¹⁴ and the supertransferred hyperfine field, H_{STHF} .¹⁵ The H_{eff} at a lattice site is primarily due to the core polarization of its site ion. But its variation is due to that of the supertransferred hyperfine field. We analyze our results in terms of H_{STHF} . In both systems it is found that $H_{\text{eff}}(B)$ remains almost constant whereas $H_{\text{eff}}(A)$ decreases with the increase of Ti^{4+} concentration. We attribute this to the fact that all the Ti^{4+} ions occupy solely the *B* site. We give below our argument in favor of these conclusions.

In the present series of ferrites, $\text{Ni}_{1-y+x}\text{Zn}_y\text{Ti}_x\text{Fe}_{2-2x}\text{O}_4$, let x Ti^{4+} ions be distributed over *A* and *B* sites in such a way that z Ti^{4+} ions, because of charge balance, replace z Fe^{3+} ions at the *A* site; $(x-z)$ Ti^{4+} ions and x Ni^{2+} ions replace $(2x-z)$ Fe^{3+} ions at the *B* site. According to this, the ionic distribution follows the structural formula $(\text{Zn}_y^{2+}\text{Fe}_{1-y-z}^{3+}\text{Ti}_z^{4+})_A(\text{Ni}_{1-y+x}^{2+}\text{Fe}_{1+y-2x+z}^{3+}\text{Ti}_{x-z}^{4+})_B\text{O}_4^{2-}$. According to the assumptions of Néel's molecular field theory, the *A-B* superexchange interactions are stronger than the *A-A* or the *B-B* superexchange interactions. Zn^{2+} and Ti^{4+} , being diamagnetic, do not participate in the magnetic superexchange interaction. Since the $\text{Fe}_A^{3+}-\text{O}^{2-}-\text{Fe}_B^{3+}$ superexchange interaction is stronger than the $\text{Fe}_A^{3+}-\text{O}^{2-}-\text{Ni}_B^{2+}$ superexchange interaction,¹⁶ the effective magnetic field is primarily due to the average $\text{Fe}_A^{3+}-\text{O}^{2-}-\text{Fe}_B^{3+}$ magnetic bonds per Fe^{3+} ion. According to the above ionic distribution, the tetrahedral Fe^{3+} ions have, on the average, $(1+y-2x+z)/2$ of their intersublattice magnetic bonds with Fe^{3+} ions at the octahedral site and $(1-y+x)/2$ of their intersublattice magnetic bonds with Ni^{2+} ions. On the other hand, the octahedral Fe^{3+} ions have, on the average, $(1-y-z)$ of their intersublattice magnetic bonds with Fe^{3+} ions at the *A* site. Since for a particular concentration of Zn (i.e., y is constant) there is no appreciable change in H_{eff} at the *B* site with the Ti^{4+} addition, we conclude that z is zero and all the Ti^{4+} ions occupy the *B* site.

Looked at from a different vantage point, the observed variation of $H_{\text{eff}}(A)$ with Ti^{4+} concentration can also be understood to arise from change in the supertransferred

hyperfine field. The supertransferred hyperfine field at the Fe^{3+} ion at the A site is due to the spin transfer from the d orbitals of the nearest-neighbor cations (i.e., belonging to the B sublattice) through the ligand anions to the s orbitals of the Fe_A^{3+} ion under consideration. Thus the supertransferred field at the A site will depend on the magnetic moment of the B site. All the nonmagnetic Ti^{4+} ions occupy the B site, thereby reducing the magnetization M_B ; this, in turn, reduces the supertransferred hyperfine field at the A site. Similarly, it can be argued that the supertransferred hyperfine field at the B site should remain constant as the magnetization M_A does not change, since Ti^{4+} ions enter only at the B site.

In Fig. 5 we have shown the variation of full width at half maximum (FWHM) of the Mössbauer absorption peak with Ti^{4+} concentration for Ti^{4+} -substituted $\text{Ni}_{0.7}\text{Zn}_{0.3}\text{Fe}_2\text{O}_4$ ferrite. At 295 K, Γ_B remains almost constant at a value of 0.775 ± 0.003 mm/sec, whereas at 77 K it drops to 0.610 ± 0.004 mm/sec and remains almost constant at that value as the concentration of Ti^{4+} increases from $x=0.00$ to 0.08. The FWHM of the tetrahedral component of the spectrum, Γ_A , at 295 K, increases from 0.561 ± 0.004 mm/sec to 0.675 ± 0.004 mm/sec as the concentration of Ti^{4+} ions increases from $x=0.00$ to 0.08. Γ_A at 77 K is 0.492 ± 0.004 mm/sec for the zero concentration of Ti^{4+} and it increases up to 0.550 ± 0.003 mm/sec for $x=0.08$. The values of Γ_A and Γ_B at 295 and 77 K of our samples with zero concentration of Ti^{4+} are consistent with the values reported by Daniels and Rosencwaig.¹²

In Ti^{4+} -substituted $\text{Ni}_{0.6}\text{Zn}_{0.4}\text{Fe}_2\text{O}_4$ ferrite, at 295 K, Γ_B remains almost constant at a value of 1.150 ± 0.004 mm/sec as the concentration of Ti^{4+} increases from $x=0.00$ to 0.08. This value of Γ_B is a little less than the value ($\Gamma_B=1.2$ mm/sec) reported by Daniels and Rosencwaig¹² of $\text{Ni}_{0.6}\text{Zn}_{0.4}\text{Fe}_2\text{O}_4$ ferrite. Γ_B drops to

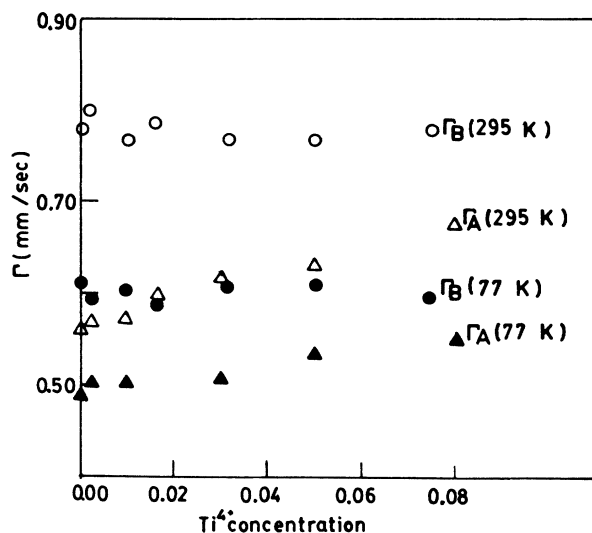


FIG. 5. Variation of full width at half maximum with Ti^{4+} concentration in $\text{Ni}_{0.7+x}\text{Zn}_{0.3}\text{Ti}_x\text{Fe}_{2-2x}\text{O}_4$ ferrite.

0.650 ± 0.003 mm/sec at 77 K and it remains almost constant at this value as the concentration of Ti^{4+} increases from $x=0.00$ to 0.08. At 295 K, Γ_A increases from 0.801 ± 0.004 to 0.955 ± 0.004 mm/sec, whereas at 77 K, it increases from 0.556 ± 0.004 to 0.691 ± 0.004 mm/sec as the concentration of Ti^{4+} increases from $x=0.00$ to 0.08.

Apart from the quadrupole broadening as discussed above there is yet another contribution to the line broadening of the Mössbauer absorption peaks. If two or more cations are present in one or both the sublattices then there will be a distribution of the values of $\langle S_z \rangle$ which results in a distribution of the values of the hyperfine magnetic field at the nucleus. This causes the broadening of the individual lines of the Mössbauer Zeeman pattern. For the sake of convenience we can call this magnetic broadening.

It is found that in both the systems the FWHM at the A site, Γ_A , increases with Ti^{4+} concentration, whereas Γ_B , the FWHM at the B site, remains almost constant. As we have seen, the change in $H_{\text{eff}}(A)$ is mainly because of the change in the contribution of the supertransferred hyperfine field at the A site which, in turn, is owing to the change in $\langle S_z \rangle$ at the B site. The increase in the value of Γ_A with Ti^{4+} concentration shows that the width of the distribution of $\langle S_z \rangle$ at B site increases as all the Ti^{4+} ions enter at the B site. On the other hand, the constancy of Γ_B is because of the fact that the width of the distribution of $\langle S_z \rangle$ at the A site is unaffected by the substitution of Ti^{4+} ions at the B site. With the decrease in temperature, the width of the distribution of $\langle S_z \rangle$ is narrowed and hence a decrease in the line broadening is expected. This is evidenced by the decrease in Γ_A and Γ_B at 77 K.

IV. STUDY OF MAGNETIZATION

In Fig. 6 we have shown the variation of magnetization, obtained from vibrating-sample magnetometer

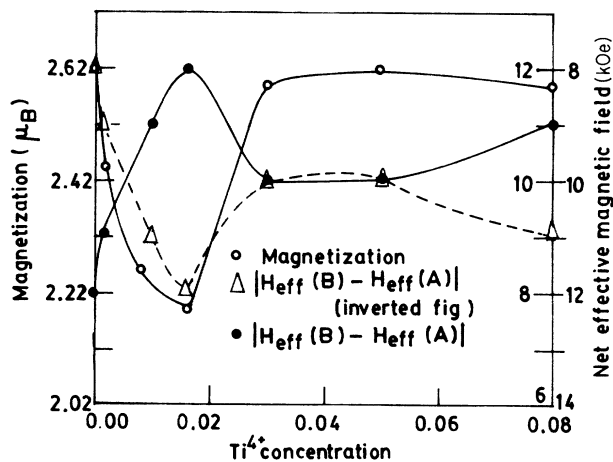


FIG. 6. Variation of magnetization and net effective magnetic field with Ti^{4+} concentration in $\text{Ni}_{0.7+x}\text{Zn}_{0.3}\text{Ti}_x\text{Fe}_{2-2x}\text{O}_4$ ferrite. The outer scale on the right is for Δ and the inner scale is for \bullet .

(VSM) measurements at 295 K, and the net effective magnetic field, $|H_{\text{eff}}(B) - H_{\text{eff}}(A)|$ with Ti^{4+} concentration on comparable scales for Ti^{4+} -substituted $\text{Ni}_{0.7}\text{Zn}_{0.3}\text{Fe}_2\text{O}_4$ ferrite. For a better visual aid in comparison between the magnetization and the net effective magnetic field an inverted scale has been chosen for the net effective magnetic field. The magnetization shows a steep fall from $2.62\mu_B$ at the zero concentration of Ti^{4+} to $2.19\mu_B$ at the Ti^{4+} concentration of $x=0.016$. It is then followed by an increase of the magnetization up to the Ti^{4+} concentration of $x=0.032$ and then the magnetization becomes almost constant up to the Ti^{4+} concentration of $x=0.08$.

For the Ti^{4+} -substituted $\text{Ni}_{0.6}\text{Zn}_{0.4}\text{Fe}_2\text{O}_4$ ferrite, we have shown the variation of magnetization and the net effective magnetic field with Ti^{4+} concentration on comparable scales in Fig. 7. It is observed that the trend in the variation of magnetization and the net effective magnetic field is the same. The magnetization falls sharply from $3.18\mu_B$ at the zero concentration of Ti^{4+} to $2.88\mu_B$ at the Ti^{4+} of $x=0.015$ followed by an increase up to $3.11\mu_B$ for $x=0.02$. The magnetization again decreases up to $2.87\mu_B$ for the Ti^{4+} concentration of $x=0.08$.

If we consider the Néel type of magnetic ordering then a linear fall of the magnetization is expected with the increase of Ti^{4+} concentration as all the Ti^{4+} ions enter at the B site only. But in both systems the magnetization curve shows nonlinear behavior. This anomalous behavior of magnetization suggests the development of canted spin structure. In a spinel ferrite each ion at the A site is surrounded by 12 B -site nearest-neighbor cations, while a cation at the B site has six B and six A ions as the nearest neighbors. Since all the nonmagnetic Ti^{4+} ions occupy the B site it is possible that the A - B superexchange interaction and the B - B superexchange interaction become comparable to each other. This will then lead to the de-

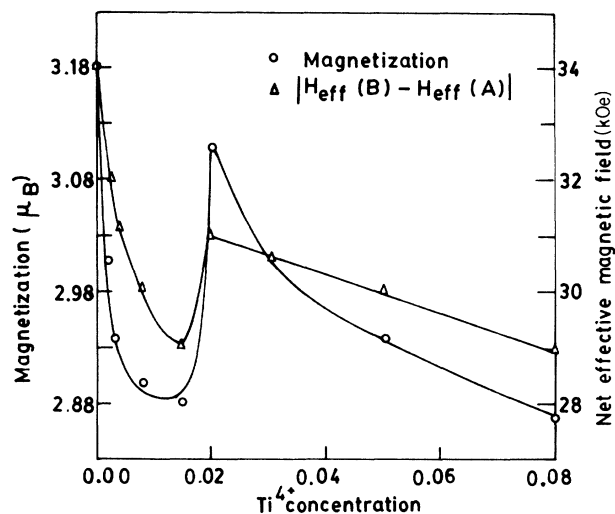


FIG. 7. Variation of magnetization and net effective magnetic field with Ti^{4+} concentration in $\text{Ni}_{0.6+x}\text{Zn}_{0.4}\text{Ti}_x\text{Fe}_{2-2x}\text{O}_4$ ferrite.

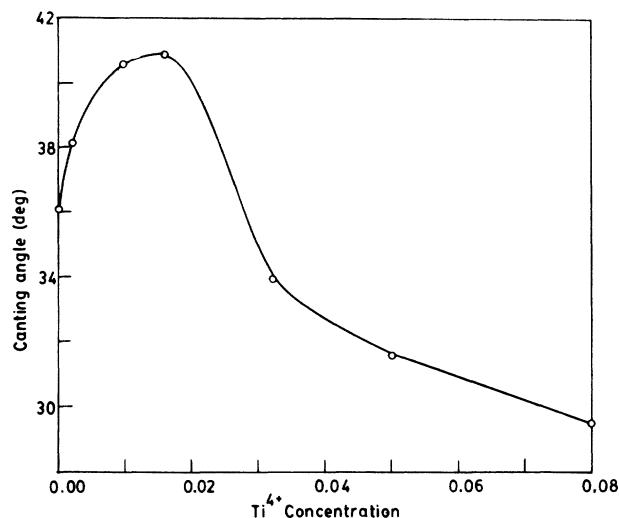


FIG. 8. Variation of canting angle with Ti^{4+} concentration in $\text{Ni}_{0.7+x}\text{Zn}_{0.3}\text{Ti}_x\text{Fe}_{2-2x}\text{O}_4$ ferrite.

velopment of canted spin structure at the B site. The variation of canting angle, as calculated from the magnetization data, with Ti^{4+} concentration are shown in Figs. 8 and 9 for the two systems.

Since in these cases the canting of spins take place at the B site, we split the B site into two sublattices B_1 and B_2 . The analysis of exchange constants in the Ti^{4+} -substituted $\text{Ni}_{1-y}\text{Zn}_y\text{Fe}_2\text{O}_4$ system is based on the modified version of Srivastava, Srinivasan, and Nandikar's¹⁷ three sublattice model. The molecular fields acting on various ions are given by

$$\begin{pmatrix} \mathbf{H}_A(\text{Fe}) \\ \mathbf{H}_{B_1}(\text{Ni}) \\ \mathbf{H}_{B_1}(\text{Fe}) \\ \mathbf{H}_{B_2}(\text{Ni}) \\ \mathbf{H}_{B_2}(\text{Fe}) \end{pmatrix} = \begin{pmatrix} \lambda_{AA} & \alpha & \beta & \alpha & \beta \\ \alpha & \gamma & \epsilon & \gamma & \epsilon \\ \beta & \epsilon & \delta & \epsilon & \delta \\ \alpha & \gamma & \epsilon & \gamma & \epsilon \\ \beta & \epsilon & \delta & \epsilon & \delta \end{pmatrix} \begin{pmatrix} A_F \mathbf{m}_A(\text{Fe}) \\ B_N \mathbf{m}_{B_1}(\text{Ni}) \\ B_F \mathbf{m}_{B_1}(\text{Fe}) \\ B_N \mathbf{m}_{B_2}(\text{Ni}) \\ B_F \mathbf{m}_{B_2}(\text{Fe}) \end{pmatrix}$$

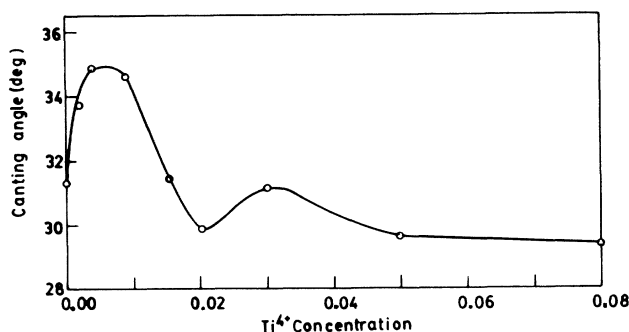


FIG. 9. Variation of canting angle with Ti^{4+} concentration in $\text{Ni}_{0.6+x}\text{Zn}_{0.4}\text{Ti}_x\text{Fe}_{2-2x}\text{O}_4$ ferrite.

Here A_F , B_N , and B_F are the concentrations of Fe^{3+} ions, Ni^{2+} ions, Fe^{3+} ions at A , $B1$ or $B2$, and $B1$ or $B2$ sublattices, respectively. The interactions $A(Fe^{3+})-A(Fe^{3+})$, $A(Fe^{3+})-B1(Ni^{2+})$, $A(Fe^{3+})-B1(Fe^{3+})$, $A(Fe^{3+})-B2(Ni^{2+})$, $A(Fe^{3+})-B2(Fe^{3+})$, $B1(Ni^{2+})-B2(Ni^{2+})$, $B1(Fe^{3+})-B2(Fe^{3+})$, $B1(Ni^{2+})-B2(Fe^{3+})$, and $B1(Fe^{3+})-B2(Ni^{2+})$ are represented by the molecular-field coefficients λ_{AA} , α , β , α , β , γ , δ , ϵ , and ϵ , respectively. And

$$\begin{aligned} \mathbf{m}_{B1} \cdot \mathbf{m}_A &= -|\mathbf{m}_{B1}| |\mathbf{m}_A| \cos\phi, \\ \mathbf{m}_{B2} \cdot \mathbf{m}_A &= -|\mathbf{m}_{B2}| |\mathbf{m}_A| \cos\phi, \\ \mathbf{m}_{B1} \cdot \mathbf{m}_{B2} &= |\mathbf{m}_{B1}| |\mathbf{m}_{B2}| \cos(2\phi). \end{aligned} \quad (2)$$

Minimizing the total magnetic interaction energy for the canting model the expression for the Yafet-Kittel angle comes out to be

$$\cos\phi = \frac{23\alpha A_F B_N + 50\beta A_F B_F}{21.16\gamma B_N^2 + 96\epsilon B_N B_F + 100\delta B_F^2}. \quad (3)$$

From the observed variation of the canting angle with concentration it is possible to evaluate the molecular-field constants. But as pointed out by Satya Murthy *et al.*¹⁸ a small error in the value of the Yafet-Kittel angles can lead to large variations in the field constants. This fact is also vindicated by Misra.¹⁹ So we choose to reverse the direction of action. We started with J values reported by Khan, Misra, and Das¹ for $Ni_{1-y}Zn_yFe_2O_4$ and converted them to molecular-field constants using the relation

$$\lambda_{A-B} = \frac{2Z_{AB}J_{A-B}}{N_B g_A g_B \mu_B^2}, \quad (4)$$

where Z_{AB} is the number of nearest neighbors of B type

surrounding the A type, N_B is the number of B -type ions per formula unit, and g_A and g_B are the gyromagnetic ratios for A and B ions, respectively. Using the information that (i) an octahedral ion has six nearest-neighbor tetrahedral ions, (ii) a tetrahedral ion has 12 nearest-neighbor octahedral ions, (iii) an octahedral ion has six nearest-neighbor octahedral ions and, (iv) a tetrahedral ion has four next-nearest-neighbor tetrahedral ions, we got a set of α , β , and λ_{AA} . These parameters were adjusted with the help of a computer program using Eq. (3) until we got the best-fitted value of $\cos\phi$. The molecular-field constants obtained in this manner yield the J values which are plotted in Figs. 10 and 11 for Ti^{4+} -substituted $Ni_{0.7}Zn_{0.3}Fe_2O_4$ and $Ni_{0.6}Zn_{0.4}Fe_2O_4$ ferrite, respectively. We see that all the exchange constants remain almost unchanged except $J_{Ni^{2+}(B)-Ni^{2+}(B)}$. In the same figures, we have also shown the variation of lattice parameter, obtained from x-ray data at 295 K, with Ti^{4+} concentration. We see that the change in the exchange constant $J_{Ni^{2+}(B)-Ni^{2+}(B)}$ reflects exactly the change in the lattice parameter. It is then evident that the overlap of the wave functions of the Ni^{2+} ions (through O^{2-} ions) and its change with the ion separation are basically responsible for the change in the canting of the spins and consequently the anomalous magnetization of these ferrites.

A correlation between the lattice parameter and exchange constant can also be evidenced from the work of Shiga.²⁰ Dionne²¹ has also found a change in the exchange constant by the diamagnetic substitutions.

Based on the hard-sphere model, the lattice parameter and oxygen parameter were calculated but there was no significant change in either of the parameters with the increase of titanium concentration. Thus the experimental curve for the lattice parameter could not be reproduced by simple theoretical calculations based on the hard-

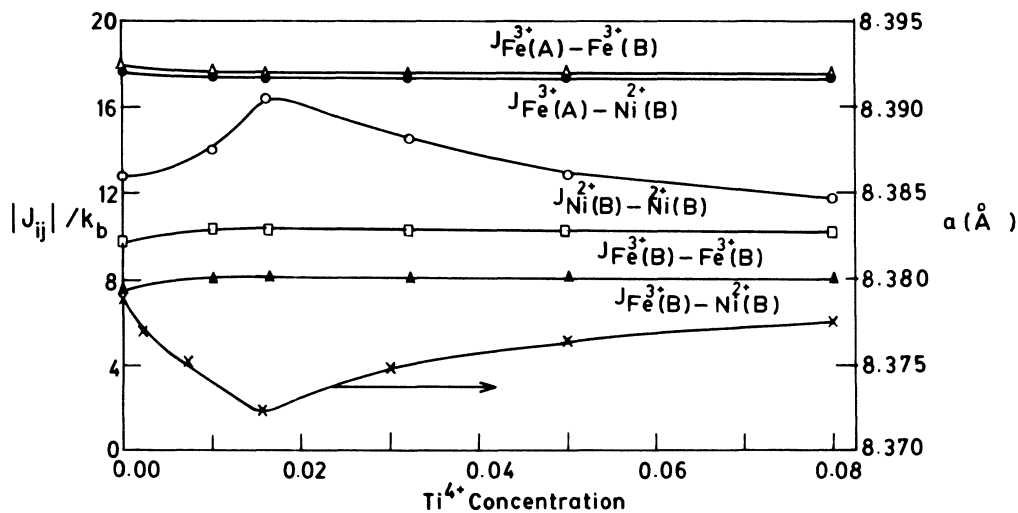


FIG. 10. Variation of exchange constants and lattice parameter with Ti^{4+} concentration in $Ni_{0.7+x}Zn_{0.3}Ti_xFe_{2-2x}O_4$ ferrite.

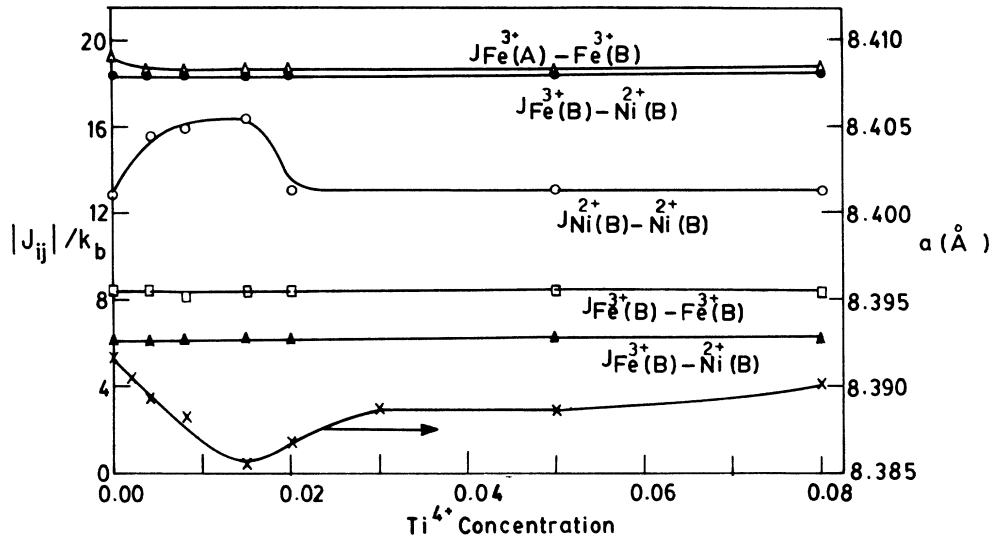


FIG. 11. Variation of exchange constants and lattice parameter with Ti^{4+} concentration in $\text{Ni}_{0.6+x}\text{Zn}_{0.4}\text{Ti}_x\text{Fe}_{2-2x}\text{O}_4$ ferrite.

sphere model. The Madelung constant was also calculated using Eq. (5) of Krupicka and Novak,²² which is based on the generalized Ewald's method used by Thompson and Grimes.²³ Here the average cationic charge was used at each lattice site. We find that the Madelung constant remains almost unchanged by the increase of titanium concentration into the lattice. Using the Born formula relating the lattice parameter with the Madelung constant, i.e.,

$$a = kM^{1/(1-n)}, \quad (5)$$

where n is a constant (usually 10), this calculation of M gave no change of a with Ti^{4+} concentration. However, using the root-mean-square charge deviation at each site gives a variation of M , and correspondingly of a . The two effects added together give a crude representation of the experimental values of the lattice parameter as a function of Ti^{4+} concentration. However, details such as the dip and the slope are not in agreement. Hence a

more sophisticated calculation of the Madelung constant is in order.

V. CONCLUSION

Thus we conclude that in Ti^{4+} -substituted $\text{Ni}_{1-y}\text{Zn}_y\text{Fe}_2\text{O}_4$ ferrite all the Ti^{4+} ions occupy the B site. The anomalous change in magnetization with the introduction of Ti^{4+} ions is due to a more complex exchange process which leads to the development of canted spin structure. The canting angle, which depends on the relative strength of various exchange constants, changes with the change of Ti^{4+} concentration. The calculation of exchange constants from canting angles shows that almost all the exchange constants remain unchanged except $J_{\text{Ni}^{2+(B)}-\text{Ni}^{2+(B)}}$. We propose that the change of these exchange constants is basically due to the variation in the overlap of the wave functions of the neighboring $\text{Ni}^{2+}-\text{O}^{2-}-\text{Ni}^{2+}$ ions caused by the change in lattice parameter.

*Also at Department of Metallurgy, Indian Institute of Technology, Kanpur 208 016, Uttar Pradesh, India.

¹D. C. Khan, M. Misra, and A. R. Das, *J. Appl. Phys.* **53**, 2722 (1982).

²D. C. Khan and M. Misra, *Bull. Mater. Sci.* **17**, 253 (1985).

³A. R. Das, V. S. Ananthan, and D. C. Khan, *J. Appl. Phys.* **57**, 4189 (1985).

⁴C. Prakash and J. S. Baijal, *Solid State Commun.* **50**, 557 (1984).

⁵J. S. Baijal and C. Prakash, in *Proceedings of the Fourth International Conference on Ferrite, Part II, San Francisco, CA, 1984*, edited by F. F. Wang (American Ceramic Society, Columbus, OH, 1985), p. 187.

⁶R. K. Puri, L. Atmaram, and K. H. Rao, in Ref. 5, p. 199.

⁷S. Margulies and J. R. Ehrman, *Nucl. Instrum. Methods* **12**, 131 (1961).

⁸P. R. Edward, C. E. Johnson, and R. J. P. Williams, *J. Chem. Phys.* **47**, 2074 (1967).

⁹E. Simanek and Z. Sroubek, *Phys. Rev.* **163**, 275 (1967).

¹⁰R. V. Pound and G. A. Rebka, *Phys. Rev. Lett.* **4**, 274 (1960).

¹¹B. D. Josephson, *Phys. Rev. Lett.* **4**, 341 (1960).

¹²J. M. Daniels and A. Rosencwaig, *Can. J. Phys.* **48**, 381 (1970).

¹³E. Matthias, W. Schneider, and R. M. Steffen, *Phys. Rev.* **125**, 261 (1962).

¹⁴L. Néel, *Ann. Phys. (Leipzig) [Folge 6]* **3**, 137 (1948).

¹⁵F. Van der Woude and G. A. Sawatzky, *Phys. Rev. B* **4**, 3159 (1971).

¹⁶S. Geller, H. J. Williams, R. C. Sherwood, and G. P. Espinose, *J. Phys. Chem. Solids* **23**, 1525 (1962).

¹⁷C. M. Srivastava, G. Srinivasan, and N. G. Nandikar, *Phys. Rev. B* **19**, 499 (1979).

- ¹⁸N. S. Satya Murthy, M. G. Natera, S. I. Youssef, R. J. Begum, and C. M. Srivastava, *Phys. Rev.* **181**, 969 (1969).
- ¹⁹M. Misra, Ph.D. thesis, Indian Institute of Technology, Kanpur, India, 1981.
- ²⁰M. Shiga, in *Magnetism and Magnetic Materials—1973 (Boston)*, Proceedings of the 19th Annual Conference on Magnetism and Magnetic Materials, AIP Conf. Proc. No. 18, edited by C. D. Graham and J. J. Rhyne (AIP, New York, 1974), Pt. 1, p. 463.
- ²¹G. F. Dionne, *J. Appl. Phys.* **41**, 4874 (1970).
- ²²S. Krupicka and P. Novak, in *Ferromagnetic Materials*, edited by E. P. Wohlfarth (North-Holland, Amsterdam, 1982), Vol. 3, p. 207.
- ²³P. Thompson and N. W. Grimes, *Philos. Mag.* **36**, 501 (1977).